the existence of the double cone. The geometry of the apex of the cone is shown in Figure 18. Note that because of the torsional angles, all the π bonds are completely broken.

IV. Conclusions

In this work we have demonstrated the existence of real conical intersections on the potential surfaces for two "textbook" pericyclic reactions. While we have found only one point on the $n - 2$ dimensional hyperline, this demonstrates that such topological features do exist.

The common assumption in organic photochemistry is that one of the central features in the mechanism of an excited-state pericyclic reaction is the existence of an avoided surface crossing the allows for the occurrence of a radiationless jump from S_1 to S_0, which is controlled by the gap between S_1 to S_0. On the other hand, the role of conical intersections on the rate of intersystem crossing seems to be widely recognized by dynamicists. Thus, a reaction that starts out on S_1 may cross directly to the ground-state surface via the conical intersection and thus the mechanism is controlled not by the S_1 to S_0 gap but rather by the presence of minima and transition states on S_0 and S_1 themselves. For the 2 + 2 cycloaddition reaction considered in this work, the biradicaloid structure on the excited-state surface is not a minimum at all but rather a transition structure with a transition vector that points to the upper part of the double cone (where return to S_0 is fully efficient). Similarly, on the S_1 surface for the electrocyclic reaction of butadiene, at the geometry of the transition state for the ground-state reaction, there is a downhill direction leading again to a conical intersection. Thus, on the S_1 surface, for geometries in the region of ground transition structures, the crossing is indeed avoided; however, a real crossing occurs at other geometries that can be predicted qualitatively by using eq 10.

Acknowledgment. This work was supported (in part) by the Science and Engineering Research Council (UK) under Grant GR/F/48029 and GR/E/4499.4.

Registry No. Ethylene, 74-85-1; *cis*-butadiene, 106-99-0.

Molecular Dynamics Simulation of a Dilute Aqueous Solution of Benzene

Per Linse

Contribution from Physical Chemistry 1, Chemical Center, University of Lund, P.O. Box 124, S-221 00 Lund, Sweden. *Received June 20, 1989*

Abstract: A dilute aqueous solution of benzene has been investigated by means of molecular dynamics simulations. The obtained preferential orientation of water molecules in the first hydration shell of benzene due to the aromaticity confirms previous results performed with different water potentials. Despite the preferential water orientation, the hydrogen-bonded network is enforced, as typically found for hydration of apolar solutes. The translational motion of benzene is slowed down by 25% and the anisotropic reorientational motion is increased 4 times as compared to pure benzene as a consequence of a more rigid and compressed oblate cage formed by the surrounding water molecules.

The generally accepted picture of hydrophobic hydration, arising both from experiment and from computer simulation, is that the loose network of hydrogen bonds is strengthened around the nonpolar solute, giving a more ordered water structure.[1-3] On the other hand, the interaction between an ion and water is quite different. The prevalent picture of ions in aqueous solutions stems from the work of Gurney[4] and Frank and Wen.[5] In this case, the orientation of water molecules close to the ion is goverened by the ion–water interaction, and the network of hydrogen bonds is partially destroyed.

A wealth of detailed information on the structure of water around a nonpolar solute molecule and the dynamics has been provided by Monte Carlo (MC) and molecular dynamics (MD) techniques. The interest spans the whole range from small, often spherical, solutes to more complex molecules such as fragments of biomolecules.[6-14] The aqueous hydration of benzene is of special interest since the typical hydrophobic hydration of apolar species may be altered by the presence of the aromaticity. The hydration of benzene is also of relevance for the hydration of other unsaturated ring structures, as in some amino acids and the nucleotide bases.

Dilute aqueous solutions of benzene have been the subject of investigations by Ravishanker, Mehrota, Mezei, and Beveridge[12] and by Linse, Karlström, and Jönsson.[11] The same water but different benzene–water potentials were used in these studies, and since MC technique was employed, only static information was provided. The results showed that the benzene was surrounded by a primary hydration shell of ≈23 water molecules. Ravishanker et al.[12] concluded that the hydration of benzene is consistent with that found for alkanes except for two water molecules, one on each side of the benzene plane, which showed a weak hydrogen bond

(1) Franks, F. *Water—A Comprehensive Treatise*; Franks, F., Ed.; Plenum Press: New York, 1972; Vol. 2.
(2) Ben-Naim, A. *Water and Aqueous Solutions*; Plenum Press: New York, 1972.
(3) Tanford, C. *The Hydrophobic Effect*, 2nd ed.; Wiley: New York, 1980.
(4) Gurney, R. W. *Ionic Process in Solutions*; McGray-Hill: New York, 1953.
(5) Frank, H. S.; Wen W. Y. *Discuss. Faraday Soc.* **1957**, *24*, 133.
(6) Swaminathan, S.; Harrison, S. W.; Beveridge, D. L. *J. Am. Chem. Soc.* **1978**, *100*, 5705.
(7) Geiger, A.; Rahman, A.; Stillinger, F. H. *J. Chem. Phys.* **1979**, *70*, 263.
(8) Geiger, A. *Ber. Bunsenges. Phys. Chem.* **1981**, *85*, 52.
(9) Alagona, G.; Tani, A. *J. Chem. Phys.* **1980**, *72*, 580.
(10) Jorgensen, W. L. *J. Chem. Phys.* **1982**, *77*, 5757.
(11) Linse, P.; Karlström, G.; Jönsson, B. *J. Am. Chem. Soc.* **1984**, *106*, 4096.
(12) Ravishanker, G.; Mehrotra, P. K.; Mezei. M.; Beveridge, D. L. *J. Am. Chem. Soc.* **1984**, *106*, 4102.
(13) Belch, A. C.; Berkowitz, M.; McCammon, J. A. *J. Am. Chem. Soc.* **1986**, *108*, 1755.
(14) Malinlak, A.; Laaksonen, A.; Korppl-Tommola, J. *J. Am. Chem. Soc.* **1990**, *112*. 86, and references citated therein.

0002-7863/90/1512-1744$02.50/0

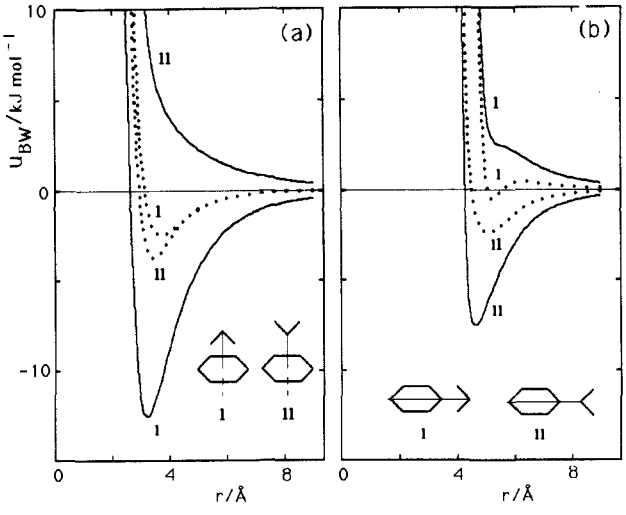

Figure 1. Benzene–water potential energy curves along the C_6 (a) and a C_2 (b) axis of benzene with the water dipole vector parallel to the axis with hydrogens pointing toward or away from the benzene. The full curves denote the full potential, whereas the dotted curves denote a modified potential where the quadrupole–dipole interaction is omitted (see text for details).

with the benzene ring. A similar conclusion was made by Linse et al.,[11] which also state that even the water molecules in the benzene plane were orientationally perturbed by the aromaticity. The calculated heats of solvating benzene in water were not reproduced in either study.

In this study the dilute aqueous solution of benzene is reexamined, now using MD technique. The motivations are 4-fold. First, the simulation time is an order of magnitude longer than normally used in hydration studies and thus the accuracy of energy and structure data is improved, which is important when studying subtle hydration effects. Second, a different water potential is used, and how the hydration depends on the potential will thus be considered. Third, the origin and the strength of the solvation structure is more thoroughly examined and a simultion where the partial charges of the benzene molecule have been switched off has also been performed. In that case, there is no electrostatic benzene–water interaction, and as we will see, the hydration structure will be different. Finally, the present study will also provide information of the dynamics of the solvated benzene, and a comparison with a liquid benzene simulation[15] will be made.

The hydration structure will receive further attention in a forthcoming report. In particular, a comparison between results from computer simulation and analytic liquid theory will be presented.[16]

Intermolecular Potential Functions

The benzene–water (BW) intermolecular potential energy function used was obtained from ab initio quantum chemical calculations using the Hartree–Fock self-consistent-field approximation, and the dispersion energy contribution was obtained by a perturbation procedure.[17] Except for the simulation of an aqueous solution of benzene,[11] the BW potential has been used to simulate the liquid–liquid benzene–water interface[18] and to calculate the intermolecular benzene–water eigenfunctions and eigenenergies for different water isotopomers.[19] One feature of the aromaticity is the permanent charge distribution of benzene, which can be expressed by an electrostatic multipole expansion where the quadrupole moment is the first nonzero term. A consequence of this charge distribution is that the BW potential energy is strongly dependent on the mutual orientation. This is illustrated in Figure 1, where the potential is shown for two different water orientations as a function of the intermolecular distance (solid curves) along the C_6 (the 6-fold symmetry axis perpendicular to the plane) and a C_2 (a 2-fold axis in the plane) axis of benzene. The global minimum is similar to the minimum structure shown in Figure 1a. It is essentially obtained from the minimum structure by tilting the water dipole vector by 35° away from the C_6 axis and its energy is lowered by 0.3 kJ mol^{-1}.[19]

In order to demonstrate the importance of the electrostatic interaction, of which the benzene quadrupole–water dipole interaction is the dominating term, a modified BW potential has been constructed by omitting the partial charges of benzene. This was carried out by setting the coefficients of the $1/r$ terms of the BW potential to zero ($A_i = 0$ in eq 10 of ref 17). It could be argued, however, that the coefficients of the $1/r^4$ terms should also be zero, since, at least formally, they correspond to charge-induced dipole interactions. But, by doing so, the potential becomes unphysical, which shows that the $1/r^4$ coefficients indeed are pure fitting quantities and strongly coupled with higher order terms. The modified potential reduces the energy difference between the different water orientations to a much smaller level, as seen in Figure 1 (dotted curves).

The TIP4P[20] potential energy function used for the water–water interaction belongs, along with the ST2,[21] MCY,[22] and SPC,[23] to the group of water potentials most frequently used in molecular simulations.

The two previous studies[11,12] of dilute aqueous solutions of benzene were performed by using different BW potentials. In this work the same BW potential is employed as used by Linse et al.,[11] whereas the potential used by Ravishanker et al.[12] displays a stronger BW attraction. Both studies used the MCY water potential. The TIP4P potential used here is known for giving a more radially structured water as compared with the MCY potential.[20,24] Hence, a weaker benzene–water structure and a smaller perturbation on the water structure due to the solute is expected in this study.

Computational Details

Two molecular dynamics simulations of a dilute aqueous solution of benzene have been performed: one using the full BW potential (labeled F), and the other using the modified BW potential (labeled M). For reference purposes a simulation of a pure water system (labeled water) was carried out as well. The MD simulations were performed with the program MOLSIM on an IBM 3090-170S VF computer. Newton's equations of motion were integrated by using the velocity form of the Verlet algorithm,[25] and the orientation of the rigid benzene and water molecules was described in a quaternion representation.[26] Periodical boundary conditions were used together with a spherical molecular cutoff and a neighbor list technique. All interactions were evaluated from a look-up table and a quadratic interpolation scheme was used. Simulation parameters are compiled in Table I.

The temperature and the pressure were kept constant by using 298 K and 0.103 MPa as external values by applying the scaling procedure of Berendsen et al.[27] with time constants of 0.1 ps. This procedure has been shown not to perturb the translational dynamics in bulk water for time constants ≤0.1 ps. The temperatures obtained from the simulations, 302 K, are 5 K above the external one. The positive difference is a consequence of the balance of a positive temperature drift mainly due to the cutoff of the water

(15) Linse, P.; Engström, S.: Jonsson, B. *Chem. Phys. Lett.* **1985**, *115*, 95.
(16) Tani, A.; Linse, P., manuscript in preparation.
(17) Karlström, G.; Linse, P.; Wallqvist, A.; Jönsson, B. *J. Am. Chem. Soc.* **1983**, *105*, 3777.
(18) Linse, P. *J. Chem. Phys.* **1987**, *86*, 4177.
(19) Linse, P. *J. Comput. Chem.* **1988**, *9*, 505.
(20) Jorgensen, W. L.; Chandrasekhar, J.; Madura, J. D.; Impey, R. W.: Klein, M. L. *J. Chem. Phys.* **1983**, *79*, 926.
(21) Stillinger, F. H.; Rahman, A. *J. Chem. Phys.* **1974**, *60*, 1545.
(22) Matsuoka, O.; Clementi, E.; Yoshimine, M. *J. Chem. Phys.* **1976**, *64*, 1351.
(23) Berendsen, H. J. C.; Postma, J. P. M.; Gunsteren, v. W. F.; Hermans, J. In *Intermolecular Forces*; Pullman, B., Ed.; D. Reidel: Dordrecht, The Netherlands, 1981; pp 331–342.
(24) Reimers, J. R.; Watts, R. O.; Klein, M. L. *Chem. Phys.* **1982**, *64*, 95.
(25) Swope, W. C.; Andersen, H. C.; Berens, P. H.; Wilson, K. R. *J. Chem. Phys.* **1982**, *76*, 637.
(26) Evans, D. J.; Murad, S. *Mol. Phys.* **1977**, *34*, 327.
(27) Berendsen, H. J. C.; Postma, J. P. M.; Gunsteren, v. W. F.; Dinola, A.; Haak, J. R. *J. Chem. Phys.* **1984**, *81*, 3684.

Table I. Simulation Parameters and Thermodynamic Results[a]

	simulation		
	F	M	water
no. of molecules			
benzene	1	1	
water	250	250	250
no. of interaction sites	1012	1012	1000
cutoff distance, Å	8.0	8.0	8.0
neighbor list update interval, fs	10.0	10.0	10.0
time step, fs	1.0	1.0	1.0
simulation time, ps	90	90	30
total CPU time, h	23.2	23.2	7.6
$\langle T \rangle$, K	302.3 ± 0.1	302.3 ± 0.1	302.4 ± 0.3
$\langle p \rangle$, MPa	0.1 ± 0.3	0.0 ± 0.3	0.5 ± 0.7
$\langle V \rangle$, Å^{-3}	7681 ± 12	7663 ± 13	7569 ± 23
$\langle U_{tot} \rangle$, kJ mol^{-1}	−10366 ± 7	−10346 ± 6	−10344 ± 7
$\langle U_W \rangle$, kJ mol^{-1}	−10304 ± 7	−10303 ± 6	−10344 ± 7
$\langle U_{BW} \rangle$, kJ mol^{-1}	−61.6 ± 0.6	−42.6 ± 0.3	
U_W^{rel}, kJ mol^{-1} [b]	40 ± 10	41 ± 10	
ΔH^∞, kJ mol^{-1} [c]	−24 ± 10	−4 ± 10	
ΔV^∞, Å^3 [d]	68 ± 16	57 ± 16	

[a] The uncertainties given are one standard deviation based on a division of the total runs into 3-ps segments, except for the last three entries where the square root of the sum of the component variances is given. [b] Relaxation internal energy of water $U_W^{rel} \equiv U_W - U_W^*$ (* refers to the pure water simulation). [c] Partial molar enthalpy of benzene (transfer of benzene from ideal gas to solution) $\Delta H \equiv H_{sol} - H_W^* - H_{gas} = (U_{BW} + U_W + pV) - (U_W^* + pV^*) - RT \approx U_{BW} + U_W^{rel} - RT$. Changes in internal degrees of freedom have been neglected. [d] Partial molar volume of benzene $\Delta V \equiv V - V^*$.

dipole–dipole interaction and the rate of cooling, which is related to the difference of the desired and momentary temperature. The pressure is much less affected and remains at 0.1 MPa within the statistical uncertainty.

Results and Discussion

Thermodynamics. Table I shows primary results of the three simulations as well as calculated relaxation internal energy of water, partial molar enthalpy, and partial molar volume of benzene in aqueous solution. The mole fraction of benzene is 0.003 and the partial molar quantities will be regarded as corresponding at infinitely diluted solution. The use of a more diluted system by increasing the number of water molecules leads to less precise molar quantities, since they are affected by fluctuations that are approximately proportional to the square root of the number of particles. Hence, the mole fraction used is regarded as a good compromise.

The experimental molar enthalpy of transferring benzene from the ideal gas to an infinitely dilute aqueous solution, ΔH^∞, at 303 K is −29.9 ± 0.1 kJ mol^{-1}.[28] The corresponding calculated value is −24 ± 10 kJ mol^{-1} where the uncertainty arises almost completely from the relaxation energy of water, $\langle U_W^{rel} \rangle$ (the difference in water internal energy between aqueous solution and pure water). A comparison among the calculated molar enthalpies, −24 (here), −95 (ref 11, simulation 2b), −290 to −200 kJ mol^{-1},[12] with the experimental one shows that the present study is a significant improvement. The difference, +71 kJ mol^{-1}, between the present ΔH^∞ and that of Linse et al.[11] stems almost completely from the relaxation energy of water, +40 (here) and −24 kJ mol^{-1} (ref 11). The difference in the total BW interaction energy, $\langle U_{BW} \rangle$, is only 7.4 kJ mol^{-1}. Since the same BW potential was used, the less negative $\langle U_{BW} \rangle$ obtained here reflects the smaller possibility of the TIP4P water molecules to adopt favorable positions with respect to benzene as compared to the MCY water. The even more negative ΔH^∞ obtained by Ravishanker et al.[12] is mainly due to a much more negative BW interaction energy, $\langle U_{BW} \rangle$ = −250 kJ mol^{-1}.

A number of calculated partial molar enthalpies of apolar solutes in water have been reported. Other related studies have been made by Swanubathan et al.,[6] Alagona and Tani,[9] and Jorgensen[10] dealing with aqueous solutions of methane, argon, and *n*-butane, respectively. In all of these investigations a typical hydrophobic hydration shell was developed. However, the former two gave too negative partial molar enthalpies as compared with experimental data; the difference ranges from −25 to −50 kJ mol^{-1}. Since the solute–water interaction is at most of the order of 10 kJ mol^{-1}, the discrepancy has mainly to be attributed to the relaxation energy of water. On the contrary, the reported partial molar enthalpy by Jorgensen was ≈0 kJ mol^{-1}, which is 25 kJ mol^{-1} too high as compared with experimental data.[29] Since Swanubathan et al., Alagona and Tani, as well as Ravishanker et al. and Linse et al. used the MCY potential (at experimental density), it seems that this water potential systematically give a too negative relaxation energy upon solvation of an apolar solute. On the other side, the use of the TIPS2 (similar to TIP4P) potential by Jorgensen and the TIP4P potential in this investigation tends to give reasonable or too positive partial molar enthalpies. This is supported by ΔH^∞ = −4 kJ mol^{-1} in the case of no partial charges of benzene; see Table I (the value is estimated to be 15 kJ mol^{-1} too high). To summarize, these results indicates that the TIP4P water potential gives more satisfactory, albeit too positive, solubility enthalpies of apolar solutes than what the MCY potential does. This conclusion is not necessarily transferable to solution of ions, since the direct ion–water interaction is of another magnitude and the perturbation of the water structure is different.

Although also with large uncertainty, the calculated partial molar volume of benzene at infinite dilution (68 ± 16 cm^3 mol^{-1}) compares reasonably favorably with recent experimental data (84 ± 1 cm^3 mol^{-1}).[30]

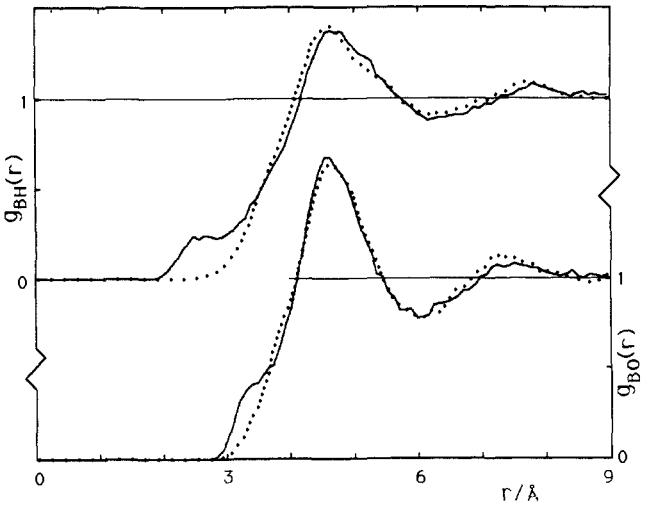

Figure 2. Radial distribution functions for benzene (center-of-mass)–oxygen (lower set, right ordinate) and benzene–hydrogen (upper set, left ordinate) pairs obtained with the full BW potential (solid curves) and the modified BW potential (dotted curves). The sets are displaced one unit, and the thin solid lines refer to isotropic distributions.

Structure. The hydration of benzene is investigated by radial distribution functions (rdf) and angular distribution functions (adf). The benzene (center-of-mass)–oxygen, g_{BO}, and benzene–hydrogen, g_{BH}, rdfs are shown in Figure 2. The four BW atom–atom rdfs will be given elsewhere.[16] The amplitude and the location of the first maximum of g_{BO} from the F simulation, 1.7 and 4.6 Å, respectively, differ considerably from those previously obtained, 2.1 and 4.4 Å,[11] and 2.8 and 4.4 Å.[12] Moreover, Linse et al. and Ravishanker et al. also found a well developed secondary hydration shell, while in this simulation the second shell could barely be discerned (see Figure 2). Thus, the less structured MCY water allows a considerably stronger layer structure around the benzene as compared to the stronger structured TIP4P water. The more attractive BW potential employed by Ravishanker et

(28) Tucker, E. E.; Lane, E. H.: Christian, S. D. *J. Solution Chem.* **1981**, *10*, 1.

(29) Abraham, M. H. *J. Chem. Soc., Faraday Trans 1* **1984**, *80*, 153.

(30) Makhatadze, G. I.; Privalov, P. L. *J. Chem. Thermodyn.* **1988**, *20*, 405.

al. results in an even more developed water layering. Despite these differences the number of water molecules in the first hydration shell (counted up to the first minimum of g_{BO}) are similar, viz. 27, 23, and 23, respectively, which merely reflects the similar molecular volume of water.

The close similarity beyond 3.5 Å of the two g_{BO} as well as of the two g_{BH}, shown in Figure 2, suggests that the hydration structures are similar in the F and M simulations. The height and the location of the first maximum as well as the first minimum of g_{BO} differ at most 0.05 and 0.1 Å, respectively. The number of water molecules in the first hydration shell ($r \leq 6.0$ Å) is also similar: 27.1 and 26.8, respectively. The only significant discrepancy occurs between 2.0 and 3.5 Å. The onset of g_{BH} at shorter distance as compared with g_{BO} in the F simulation implies that these water molecules, which are located close to the C_6 axis (cf. Figure 1 and see below), prefer to have their hydrogens oriented toward the benzene. No such preference is seen in the M simulation.

For a more detailed investigation of the hydration structure, water molecules are classified into two groups, those close to the C_6 axis ($\theta \leq 30°$ or $\theta \geq 150°$) and those close to the benzene plane ($60° \leq \theta \leq 120°$), where θ is the angle between the BW interparticle vector and the direction of the C_6 axis. The onset of g_{BO} and the location of its first maximum are 2.7 and 3.4 Å, and 3.8 and 4.7 Å, for the two groups, respectively (F simulation). The region that satisfies $\theta \leq 30°$ or $\theta \geq 150°$ *and* $r \leq 5.1$ Å ($r = 5.1$ Å is the location of the first minimum of the g_{BO} obtained from the F simulation using only water molecules satisfying $\theta \leq 30°$ or $\theta \geq 150°$) is labeled *top*, whereas the region satisfying $60° \leq \theta \leq 120°$ *and* $r \leq 6.3$ Å is labeled *side*. The average numbers of water molecules in the top region are 2.8 (F) and 2.7 (M), and in the side region 15.4 (F) and 15.3 (M). Despite the low number of molecules in the top region and concomitantly less statistical accuracy, this division will be useful to probe the different structure in these two regions.

Average orientations of water molecules in the top and side regions are presented in Figure 3 by means of angular distribution functions of the dipole vector and the OH-bond vector orientation. The corresponding adfs for the two regions from the M simulation agree with each other (within the statistical uncertainty) and only their averages are presented. Adfs have also been calculated for water molecules in the second hydration shell, $r = 6$–9 Å, but no significant preferential orientation was found from either the F or the M simulation.

Figure 3a shows that the electrical field from the partial charges of benzene tends to orient the water dipole vectors in the primary hydration shell, and in opposite ways in the two regions, as expected. The orientation effect is smaller for the side region, but appreciable for the top region (cf. Figure 1). However, the latter preferential dipole orientation is still considerably smaller than that found for water molecules in the primary hydration shell of monovalent ions in aqueous solution.[13,31] The tendency of the dipole vectors to be pointing away from the benzene in the M simulation is a consequence of the difference in the location of the onset of the repulsive core for orientations I and II, displayed in Figure 1. With a more equal onset, a more uniform distribution of cos Ψ_d would have been obtained as in previous investigations.[7,8,31]

The corresponding OH-bond vector analysis, shown in Figure 3b, reveals that in the absence of partial charges, the adf display maxima at ≈60° and ≈180°, in very good accordance with the prevailing picture of hydrophobic hydration of small solutes.[7,8,31] The water molecules have one of the four tetrahedral bond directions pointing radially outward and the other three straddle the benzene. In the presence of the partial charges, there is only a very modest change in the side region. The small increased probability of an outward pointing dipole vector is accompanied by an enhanced probability of an OH-bond vector pointing strictly away from the benzene at the expense of an oxygen lone pair; yet still the straddling is preserved. However, the situation is changed

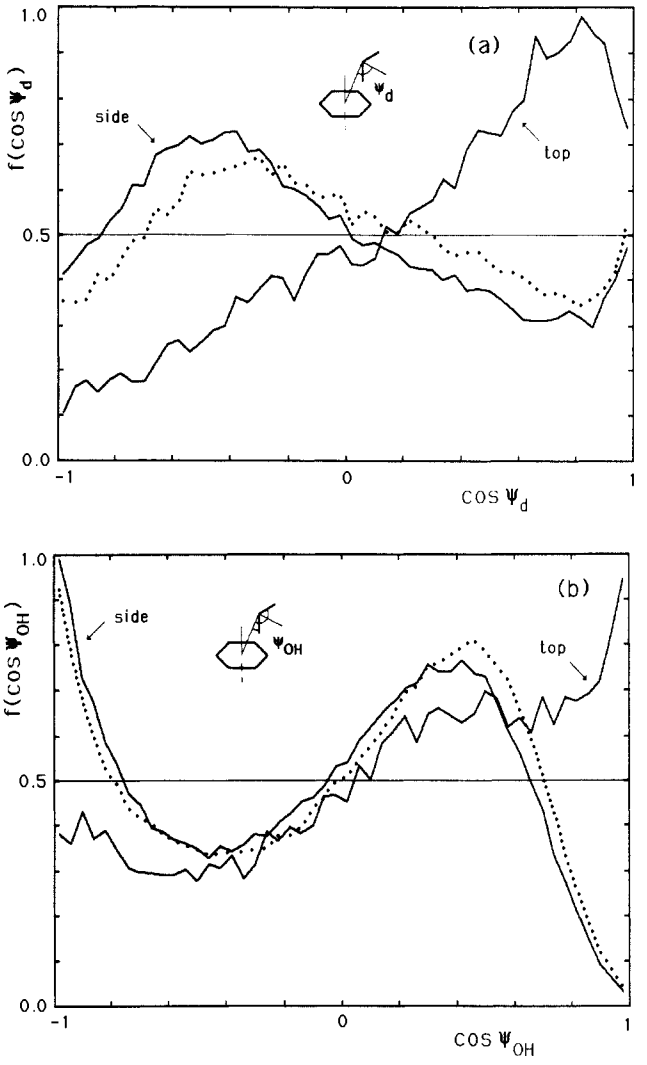

Figure 3. Angular distribution function of the interparticle–dipole vector angle (a) and interparticle–OH-bond vector angle (b) for water molecules belonging to top and side regions obtained with the full BW potential (solid curves) and the modified BW potential (dotted curves). In the latter case, since top and side functions were equal, only their averages are displayed. The thin solid lines refer to isotropic distributions.

in the top region. The maxima of the adfs at $\Psi_{OH} = 0°$ and $\Psi_d \approx 40°$ show that one OH-bond vector points radially toward the benzene. This arrangement sacrifices one possibility of hydrogen bonding, but the other three possibilities can maintain normal interaction. In this respect the situation resembles that in the first 0.5-Å water layer outside a planar and smooth hydrophobic surface.[32] However, the tendency is weaker here and the mechanisms are different. In the case of hydration of benzene, it is the electrostatic interaction, whereas in the case of the smooth surface, it is the surface itself that causes the sacrifice of one possibility of hydrogen bonding.

The water structure per se is examined by considering the number of water neighbors and hydrogen bonds as well as by adfs. The presence of a solute introduces trivial changes of the number of hydrogen bonds (and neighbors). In order to examine the inherent tendency of forming hydrogen bonds, it is instructive to use the ratio of the number of hydrogen bonds to the number of water neighbors, rather than just the number of hydrogen bonds. Typically, this ratio increases for hydrophobic hydrated water molecules,[18,32] whereas it decreases for ionic hydrated water

(31) Linse, P. *J. Chem. Phys.* **1989**, *90*, 4992.

(32) Lee, C. Y.; McCammon, J. A.; Rossky, P. J. *J. Chem. Phys.* **1984**, *80*, 4448.

(33) McCool, M. A.; Collings, A. F.; Woolf, L. A. *J. Chem. Soc. Faraday Trans. 1* **1972**, *68*, 1489.

(34) Gillen, K. T.; Griffiths, J. E. *Chem. Phys. Lett.* **1972**, *17*, 359.

Table II. Average Number of Water Neighbors within 3.5 Å from a Water Molecule, n_{NN}, and Average Number of Hydrogen Bonds with Neighbors within 3.5 Å, n_{HB}[a]

	simulation			
	F		M	
	hydr shell	bulk	hydr shell	bulk
n_{NN}	4.71	5.21	4.80	5.21
n_{HB}[b]	3.30	3.38	3.33	3.37
n_{HB}[c]	2.18	2.17	2.18	2.16
n_{HB}/n_{NN}[b]	0.701	0.649	0.694	0.647
n_{HB}/n_{NN}[c]	0.463	0.417	0.454	0.415

[a] Two water molecules are considered hydrogen bonded if their pair energy is lower than a threshold value ϵ. Averages are made for molecules belonging either to the primary hydration shell or to bulk. Data for the secondary hydration shell are equal to those in bulk and are not given. The largest uncertainties (one standard deviation) are 0.02 in the first three rows and 0.004 in the last two rows. They are based on a division of the total runs into 3-ps segments. [b] $\epsilon = -10$ kJ mol^{-1}. [c] $\epsilon = -16$ kJ mol^{-1}.

molecules.[31] The results given in Table II show that the number of hydrogen bonds is almost the same irrespective of whether benzene carries partial charges or not, and moreover, this number is equal to that of bulk. (Water molecules beyond 9-Å separation from the benzene are referred to as bulk.) However, by considering that the number of nearest neighbors available for hydrogen bonding is decreased by 9–10% in the hydration shell, an ≈8% increased tendency of forming hydrogen bonds is found. This enhancement should be compared with an increase of 30% for water molecules in the primary hydration shell at a planar smooth hydrophobic surface[32] and a reduction of typically 50% found for water molecules in the primary hydration shell of monovalent cations.[31] The same analysis has been performed in the top and side regions separately. The less demanding energy criteria of a hydrogen bond, $\epsilon = -10$ kJ mol^{-1}, gave $n_{HB}/n_{NN} = 0.69, 0.70, 0.69$, and 0.69, whereas $\epsilon = -16$ kJ mol^{-1}, gave 0.45, 0.47, 0.46, and 0.46 in the order top (F), side (F), top (M), and side (M). Hence, in the M simulation the tendency of forming hydrogen bonds is the same in the top and side regions, but a small decrease appears in the top region of the F simulation. However, it should be kept in mind that the change is small and that n_{HB}/n_{NN} in the top region is still *larger* than in bulk, and the top region is, in this respect, still *hydrophobic* hydrated.

Five adfs for reference water molecules in the primary or secondary hydration shell or in bulk have been calculated. The angles considered are the angles between dipole vector–dipole vector, interparticle vector–dipole vector, and interparticle vector–OH bond vector as well as OH···O and O···O···O angles between/among water neighbors (see ref 31 for more details). Figure 4 shows the average orientation of the OH-bond vector of water neighbors with respect to the location of the reference water molecule in bulk. The hydrogen-bonded network of a tetrahedral type is manifested by the high probabilities of $\Psi_{OH} \approx 0°$, reflecting the situation where the reference molecule acts as an electron donor, and at $\Psi_{OH} \approx 110°$ where it acts as an electron acceptor. The deviation from the distribution in bulk, shown as difference curves in Figure 4, reveals the increased tetrahedral structure in the primary hydration shell as well as the similarity of the F and M simulations. The other four adfs (not shown) also show (i) that only water molecules in the primary hydration shell are perturbed, (ii) the characteristics of hydrophobic hydration, and (iii) only small differences between the F and M simulations.

Thus, the increased tendency of forming hydrogen bonds and the stronger tetrahedral structure show clearly that benzene is hydrophobic hydrated. The presence of the quadrupole moment of benzene *does not* essentially alter the hydrogen-bonded network. The perturbation imposed on the water structure from the quadrupole–dipole interaction seems not to be strong enough to disturb the typical hydrogen-bonded network formed around a more representative hydrophobic solute as cyclohexane. Although the orientational perturbation induced by the partial charges in the top region is considerable, either the perturbation is not strong

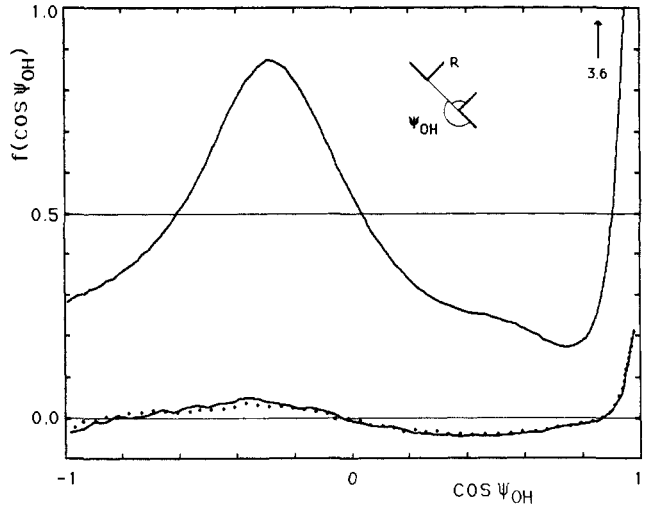

Figure 4. Angular distribution function for interparticle–OH-bond vector angle. Averages are made over water neighbors (<3.5-Å separation) from reference water molecule (labeled R) belonging to the bulk (upper solid curve), the hydration shell obtained with the full BW potential (lower solid curve), and the modified BW potential (dotted curve). The adf for bulk has been subtracted from the adfs for the hydration shell. The thin solid line at 0.5 refers to an isotropic distribution in bulk and same vertical scale applies to all curves.

enough or the number of water molecules in the region is not large enough (less than two on each side on the benzene) to significantly increase the constraint of the hydrogen-bonded network. This should be compared with the situation for hydrophilic hydrated ions where (i) all water molecules in the primary hydration shell are similarly affected, (ii) the perturbing force acting on each molecule is larger (e.g., the two lone pairs of a water molecule in the first hydration shell straddle a cation), and (iii) the more long-ranged ion–dipole interaction also affects water molecules beyond the primary hydration shell.

Dynamics. The dynamics of water is examined by considering time correlation functions averaged over water molecules initially belonging to either the primary hydrogen shell, secondary hydrogen shell, or bulk. Again, since the data for the secondary hydration shell agree with those of the bulk (within the statistical uncertainty) only data for the primary hydration shell and bulk are reported.

The exchange of water molecules initially belonging to a specified region (forming a class) is investigated by using reduced propagators. Let the propagator $P(\Gamma,t|\Gamma,0)$ be the probability that a given molecule belongs to class Γ at time t if it belonged to the same class at time zero. The reduced propagator, $\tilde{P}(\Gamma,t|\Gamma,0)$, is defined as

$$\tilde{P}(\Gamma,t|\Gamma,0) = \frac{P(\Gamma,t|\Gamma,0) - P(\Gamma,\infty|\Gamma,0)}{P(\Gamma,0|\Gamma,0) - P(\Gamma,\infty|\Gamma,0)} \quad (1)$$

with the limiting values $\tilde{P}(\Gamma,0|\Gamma,0) = 1$ and $\tilde{P}(\Gamma,\infty|\Gamma,0) = 0$. The exchange time τ_{ex} is now defined as the time integral of the reduced propagator

$$\tau_{ex} = \int_0^\infty \tilde{P}(\Gamma,t|\Gamma,0)\, dt \quad (2)$$

Reduced propagators are used to characterize the exchange of water molecules from the benzene hydration shell, as well as the exchange of molecules in hydration shells (<3.5 Å separation) of water molecules in bulk. The reduced propagators display an initial fast decay due to fast vibrational motion and an approximatively exponential behavior after ≈0.5 ps (cf. ref 31). The obtained exchange times are $\tau_{ex} = 11.7 \pm 0.5$ and 3.8 ± 0.2 ps for the benzene and water hydration shells, respectively, and are same for the F and M simulations. (The exchange times were evaluated by using eq 2 for the interval 0–10 ps with an exponential continuation using time constants obtained from the 5–10 ps interval.) Thus, the exchange rate is slowed down by a factor of

Table III. Translational Self-Diffusion Coefficients, $D/10^{-9}$ m^2 s^{-1}, for Benzene and Water (Initially Belonging either to the Hydration Shell or to Bulk)[a]

	simulation		
	F	M	benzene[b]
water (hydr shell)	2.9 (3.1)	3.0 (3.2)	
water (bulk)	3.4 (3.5)	3.3 (3.5)	
benzene	1.8 (2.0)	1.7 (2.4)	2.6 ± 0.3

[a] Calculated from mean square displacements and from velocity time correlation functions (the latter in parentheses). The interval 1–10 ps is used for the msd fits and 0–1 ps for the vtcf integrations. Estimated uncertainties are 0.1 for water, whereas 0.2 (msd) and 0.3 (vtcf) are for benzene. [b] Simulated value from ref 15 recalculated from 312 to 302 K by using experimental temperature dependence according to ref 33, $D(302) = 0.68D(312)$.

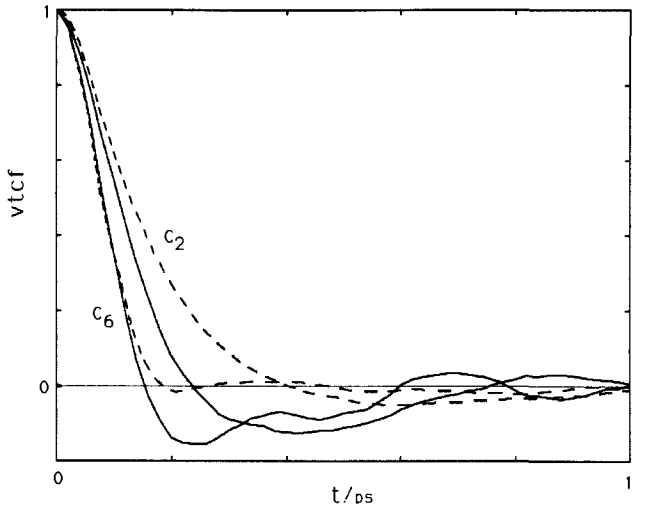

Figure 5. Velocity time correlation function along the C_6 axis (two faster decaying curves) and along the C_2 axis (two slower decaying curves) of benzene in aqueous solution at 303 K (solid curves) and in pure benzene at 312 K from ref 15 (dashed curves).

3 as compared with that from a water hydration shell in bulk. Since water molecules are engaged in a similar number of hydrogen bonds irrespective of whether it is benzene hydrating or in bulk, the main reduction of the exchange time is an obstruction effect. The negligible effect from the partial charges shows that the exchange is dominated by water–water interactions and obstruction. This is anticipated since the average BW pair energy for a primary hydrated water molecule is as low as −1.9 and −1.3 kJ mol^{-1} in the F and M simulations (cf. the water–water hydrogen bond energy of −10 to −20 kJ mol^{-1}).

The translational motion is analyzed in terms of mean square displacement (msd) and velocity time correlation functions (vtcf). The translational diffusion coefficient D can be calculated either from the long time limit of the msd or from the integral of the vtcf.[15] Since the correlation time of the vtcf is more than 1 order of magnitude smaller than τ_{ex}, it is possible to obtained D for molecules located in the hydration shell by using the linear behavior of the msd between ≈1–10 ps. Table III shows that the translational self-diffusion of benzene is similar in the F and M simulations and ≈25% reduced as compared to pure benzene simulation. Experimental values are difficult to obtain due to the low solubility. However, by considering the Stoke–Einstein relation $D \approx 1/\eta$ as well as $\eta(W) = 0.80$ and $\eta(B) = 0.56$ cP at 303 K, the obtained result is reasonable. Table III also shows that the water self-diffusion is slightly reduced in the hydration shell, approximatively 10%.

Figure 5 shows calculated parallel and perpendicular components (with respect to the C_6 axis) of the vtcf of benzene in aqueous solution and in pure benzene. In both cases the correlation times of the vtcf for the parallel component is about twice that for the perpendicular one. This agrees reasonably with the estimated cross sections.[15] However, the vtcf for benzene in aqueous solution, in particular the parallel component, becomes negative after ≈0.2 ps (cage effect), i.e., the direction of the translation is reversed. This is in contrast to bulk benzene where the vtcfs decay much more exponentially. The M simulation shows cage effects (not shown) similar to the F simulation.

Table IV. Rotational Diffusion Coefficients, θ/ps, for Benzene[a]

	simulation		
	F	M	benzene[b]
$\theta_\perp$	0.06 (0.04)	0.10 (0.13)	0.09 (0.12)
$\theta_\parallel$	0.6 (0.5)	0.5 (0.6)	0.25 (0.27)
$\theta_\parallel/\theta_\perp$	10	5	2.5

[a] Calculated from angular time correlation functions by use of the first Legendre polynomial and from angular velocity time correlation functions (the latter in parentheses). The interval 1–4 ps is used for least-squares exponential fits of the atcfs and 0–1.5 ps for the avtcf integration. Estimaed uncertainties are 10% and 20%, respectively. [b] Simulated data from ref 15 recalculated from 312 to 302 K by using experimental temperature dependence according to ref 34, $\theta_\perp(302) = 0.88\theta_\perp(312)$ and $\theta_\parallel(302) = 1.0\theta_\parallel(312)$.

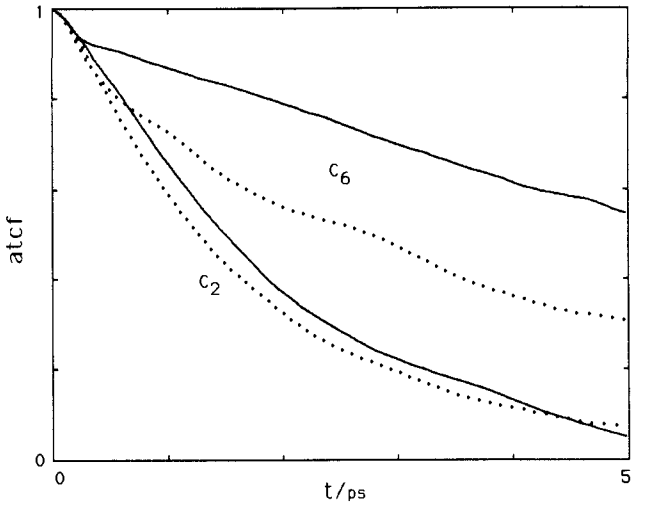

Figure 6. Angular time correlation function for the C_6 axis (upper two curves) and the C_2 axis (lower two curves) of benzene with the full BW potential (solid curves) and the modified BW potential (dotted curves).

The rotational motion is analyzed by employing angular time correlation functions (atcf) and angular velocity time correlation functions (avtcf) of the molecular principal axes. For a diffusive rotational motion, the rotational diffusion coefficients of a symmetric top, $\theta_\parallel$ and $\theta_\perp$, can be calculated either from an exponential fit of the two atcfs or from the integral of the avtcfs.[15] Table IV shows calculated rotational diffusion coefficients of benzene in aqueous solution and in pure benzene. Whereas $\theta_\parallel$ is equal for the F and M simulations and twice as fast as in pure benzene, $\theta_\perp$ from the F simulation is less that half of the value from the M simulation, which is similar to that of pure benzene. The ratio $\theta_\parallel/\theta_\perp$, a measure of the anisotropy of the rotation, is thus approximately increased by a factor of 2 in each step: in the order pure benzene, aqueous solution (M), aqueous solution (F). This shows that although the solute is the same, the reorientation anisotropy may depend strongly on the solvent.

Figure 6 shows the two components of the atcfs from the F and M simulations. As for pure benzene the perpendicular components start to fall faster after the first 0.5 ps. The figure clearly shows the much slower reorientation *of* the C_6 axis due to the more sluggish reorientation *around* the C_2 axes, which is more pronounced in the F simulation.

The two components of the avtcf of benzene in aqueous solution and in pure benzene are shown in Figure 7. Both parallel components exhibit a monotonic decay, well described within a stochastic Langevin model. However, the time constant $\theta_\parallel$ for benzene is twice as large—the spinning is less hindered by friction exerted by surrounding molecules—in aqueous solution. The perpendicular component in aqueous solution shows a much more

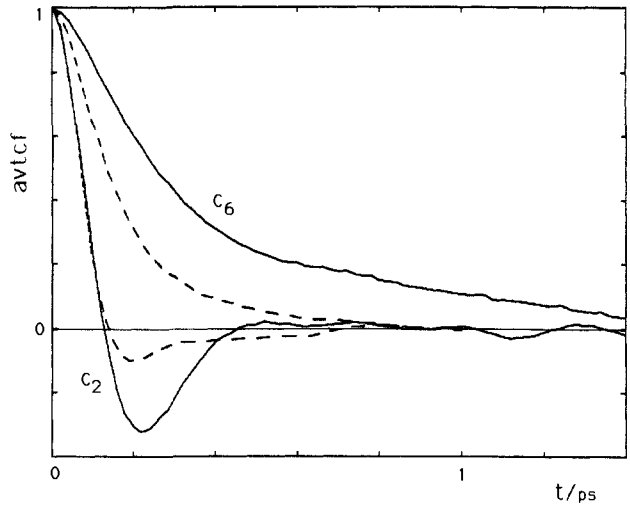

Figure 7. Angular velocity time correlation function for the C_6 axis (upper two curves) and the C_2 axis (lower two curves) of benzene in aqueous solution at 303 K (solid curves) and in pure benzene at 312 K from ref 15 (dashed curves).

Table V. Reorientational Correlation Times, τ/ps, for the Three Principal Water Axes[a]

	simulation			
	F		M	
axis[b]	hydr shell	bulk	hydr shell	bulk
x'	3.0	2.5	2.8	2.6
y'	4.2	3.5	4.1	3.5
z'	3.9	3.5	4.2	3.4

[a] Averages are made for molecules initially belonging either to the hydration shell or to bulk. The reorientational correlation times are obtained from least-squares exponential fits of the atcf using the 1–5-ps interval. Estimated uncertainty is 0.1. [b] x' denotes a vector parallel to the HH vector, y' a vector perpendicular to the HOH plane, and z' a vector parallel with the dipole vector.

prominent cage effect as compared with pure benzene; in fact the avtcf is qualitatively similar to that in solid benzene at 261 K.[15] But in the M simulation the cage effect of the perpendicular component is similar to that for pure liquid benzene (not shown).

The vtcf as well as the avtcf and the rotational diffusion coefficients indicate that the translational and rotational motion of benzene is different in aqueous solution and in pure benzene. The origin of the strong tendency of reversing the rotation direction of the perpendicular component and the reduced $\theta_\perp$ has to be sought in the higher hydrogen density above and below the benzene plane promoted by the aromaticity. These hydrogens create a narrower and steeper libration potential well for the tumbling motion but leave the spinning motion unaffected. A tentative explanation of the increased spinning motion in water as compared with pure benene is that the hydrogen-bonded network spans a water cage in which the benzene spins more freely as compared with pure benzene. This picture is supported by the fact that the vtcf shows considerable sign reversal in water but not in benzene.

Finally, the reorientation of water will be considered. After the decay during the first 0.2 ps governed by fast local librations, the avtcf becomes nearly exponential during the time interval studied. The reorientational correlation times for the three principal water axes are given in Table V. There is hardly any difference between the F and M simulations. Both of them are ≈15% (an average over the three axes) longer than in bulk.

Summary

On the basis of a molecular-level simulation of a model system of a dilute aqueous solution of benzene, the energetics, structure, and dynamics have been investigated. A modified BW potential has also been used in order to examine the role of the partial charges of benzene. The present MD study employs a different water potential and is approximatively an order of magnitude longer than previous MC studies of the same system.

The use of the TIP4P water potential and the BW potential by Karlström et al. gives a significant improvement and a very satisfactory molar enthalpy and volume of solution as compared with the previous studies. The more structured TIP4P water potential gives a less developed benzene–water structure in comparison with the MCY potential.

This investigation with the present limitations, of which the most important is probably the pairwise potential assumption, shows that the hydration of benzene is similar to that of nonaromatic alkanes. The consistent picture is that the forces from the partial charges are responsible for the preferential water orientation found in the primary hydration shell. The influence is strongest above and below the benzene ring, where a water molecule tends to have one hydrogen pointing toward the benzene. However, the effect is *not* so strong that the integrity of the hydrogen-bonded network (enforced by the hydrophobic nature of benzene) is significantly disturbed.

The translational dynamics of benzene is slowed down by ≈25% as compared with pure benzene. The rotational anisotropy is increased 4-fold as a consequence of a faster spinning and slower tumbling motion. This is interpreted in terms of a more rigid and compressed oblate cage about the benzene in aqueous solution as compared with pure benzene. The dynamics of the water molecules is the primary hydration shell are slowed down by 10–15%.

Acknowledgment. This research was supported by the Swedish Natural Science Research Council.

Registry No. H_2O, 7732-18-5; PhH, 71-43-2.